Strong vertical mixing of deep water of a stratified reservoir during the Maule earthquake, central Chile (M_w 8.8)

Alberto de la Fuente,[1] Carolina Meruane,[2] Manuel Contreras,[3] Hugo Ulloa,[1] and Yarko Niño[1]

Received 12 October 2010; accepted 19 November 2010; published XX Month 2011.

[1] Vertical profiles of water temperature in Rapel reservoir (central Chile, 34° 2′ 23″ S, 71° 35′ 23″ W, 110 m.a.s.l.), recorded the hydrodynamic response of the stratified water column of the reservoir produced by the 8.8 magnitude Maule earthquake (epicentre located in 36°15′36″S, 73°14′ 20″W), showing an intense vertical mixing of deep water. The vertical mixing was characterized by changes in the potential energy of the water column and the eddy diffusivity of the mixing, and these values were used to estimate the mixing efficiency of the event. It is hypothesized that the turbulent flow that mixed the water column was mainly induced by the oscillation of the bed, although surface gravitational waves could also have contributed to the vertical mixing. So far, this is the first time that the hydrodynamic response of a reservoir during a mega-earthquake is measured and described. **Citation:** de la Fuente, A., C. Meruane, M. Contreras, H. Ulloa, and Y. Niño (2011), Strong vertical mixing of deep water of a stratified reservoir during the Maule earthquake, central Chile (M_w 8.8), *Geophys. Res. Lett.*, *38*, LXXXXX, doi:10.1029/2010GL045798.

1. Introduction

[2] On 27 February 2010, a 8.8 magnitude earthquake followed by a tsunami hit Central Chile killing in together more than 500 peoples, and causing damages in the national infrastructure amounted in several thousand of million American dollars [*Madariaga et al.*, 2010; *Kaiser and Regalado*, 2010; *Regalado*, 2010; *Lay et al.*, 2010]. Besides the consequences that a mega-earthquake has on the human activity, the released energy during the Maule earthquake and the way on which that release occurs, trigged natural phenomena that are difficult to be measured under normal conditions [*Montgomery and Manga*, 2003; *Farías et al.*, 2010]. One of these events is documented and discussed here, and corresponds to the intense vertical mixing of the stratified Rapel reservoir during the Maule earthquake.

2. Methods and Results

2.1. Field Measurements and Mixing Characterization

[3] Rapel reservoir is an artificial lake located at about 120 km from Santiago, the capital city of Chile (see Figure 1a). It was built in 1968 for hydro-power generation with a maximum water depth of 85 m near the dam [*Contreras et al.*, 1994; *Vila et al.*, 1997; *de la Fuente and Niño*, 2008]; however, reservoir sedimentation raised the bottom elevation in 30 m, being today the maximum water depth of 55 m. Water withdrawals for hydro-power generation are located at about 45 m depth, elevation at which a density interface develops during summer time [*de la Fuente and Niño*, 2008].

[4] During the Maule earthquake occurred on day 58 of 2010, a thermistor chain located at about 350 m from the dam (Figure 1b), recorded time-series of water temperature every 30 minutes at 11 different depths, with thermistors spaced each other by 5 m, such as the lowest thermistor is located below the density interface. Water depth in point of the thermistor chain location was about 54 m during Maule earthquake. Measurements during the days before and after the earthquake are shown in the contour plot of Figure 2a, in which the intense mixing in the deepest region of the lake (below 25 m depth) is observed during the Maule earthquake that is marked by the vertical dashed line. This vertical mixing is clearer seeing in Figure 2b in which time series of water temperature at 45 and 50 m depth show a strong temperature gradient of about 2°C in 5 m before the earthquake, followed by the nearly complete vertical-homogenization of the water temperature after the earthquake marked by the vertical dashed line. This vertical mixing is also shown in Figure 2c, where both vertical profiles are separated each other by 30 minutes, thus showing that vertical mixing was quite instantaneous and localized in deepest areas of the water column, while surface water densities (above 25 m depth) did not change product of the earthquake.

[5] In terms of energy budget, changes in water temperature indicate changes in the potential energy of the lake, which increases in case of a mixing event [*Fischer et al.*, 1979; *Imberger and Hamblin*, 1982; *Wüest et al.*, 2000]. Potential energy per unit of area of bed is estimated as the gravity centre elevation times the total mass of the water column [*Wüest et al.*, 2000; *Antenucci et al.*, 2000]; therefore, since the deepest waters are denser in stratified conditions, the gravity centre is deeper than in homogenous conditions, thus being required an external source of energy to induce vertical mixing [*Fischer et al.*, 1979; *Imberger and Hamblin*, 1982; *Wüest et al.*, 2000]. In case of Rapel reservoir, the potential energy per unit of bed area of the water column between the elevation of the deepest thermistor (zt) and the free surface at the elevation H, was computed by solving the integral

$$PE = \int_{zt}^{H} \rho g z \, dz, \quad (1)$$

[1]Departamento de Ingeniería Civil, Universidad de Chile, Santiago, Chile.
[2]Ingeniería y Modelación Ambiental Ltda., Santiago, Chile.
[3]Centro de Ecología Aplicada Ltda., Santiago, Chile.

0094-8276/11/2010GL045798

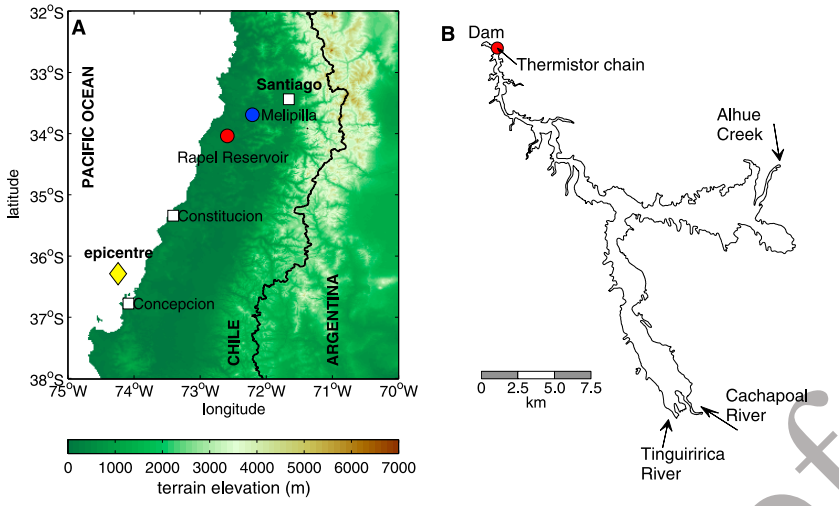

Figure 1. (a) Geographic location of Rapel reservoir, Melipilla seismological station, the earthquake epicentre and mayor cities of the area. (b) Perimeter of Rapel reservoir and arrows indicate inflows (Cachapoal and Tinguiririca rivers and Alhué creek). Red dot specifies the location of thermistor chain.

based on a trapezoidal integration, obtaining the time series of *PE* shown in Figure 3a, where it is observed that mixing due to the Maule earthquake increased the potential energy per area of bed in 0.8 kJm^{-2}. To put in context this change in potential energy per unit of area of bed, about 1% of the total energy in the internal wave field of a stratified lake may be used in raising the potential energy [*Gloor et al.*, 2000; *Shimizu and Imberger*, 2008], and the total energy per unit of area in the internal wave field induced by typhoons passing over Lake Biwa (Japan) was estimated in 0.52 kJm^{-2} [*Shimizu et al.*, 2007]. Therefore, typhoons on Lake Biwa may induce vertical mixing equivalent to 0.005 kJm^{-2} (1% of the total energy in the flow) in a timescale of days, while Maule earthquake produced mixing two order of magnitude larger in a timescale of minutes.

[6] Furthermore, the eddy diffusivity, K_ρ, which characterizes the mixing induced by the Maule earthquake, was estimated by solving the vertical diffusion equation of the water density, ρ,

$$\frac{\partial \rho}{\partial t} = \frac{\partial}{\partial z}\left(K_\rho \frac{\partial \rho}{\partial z}\right). \quad (2)$$

This equation was numerically solved following *Patankar* [1980], with the initial condition defined by the vertical profile measured before the earthquake (red line in Figure 2c), and a constant and homogeneous K_ρ was calibrated such as obtaining the best fit with measurements 30 minutes after (blue line in Figure 2c). Boundary conditions to solve (2) were no-flux boundary condition at the bottom of Rapel reservoir ($z = 0$ m, or 54 m depth during the earthquake), and, because of the water density above 25 m depth did not change during the earthquake (Figure 2c), ρ = 997.72 kg m^{-3} was imposed at z = 29 m (or 25 m depth). Furthermore, the initial

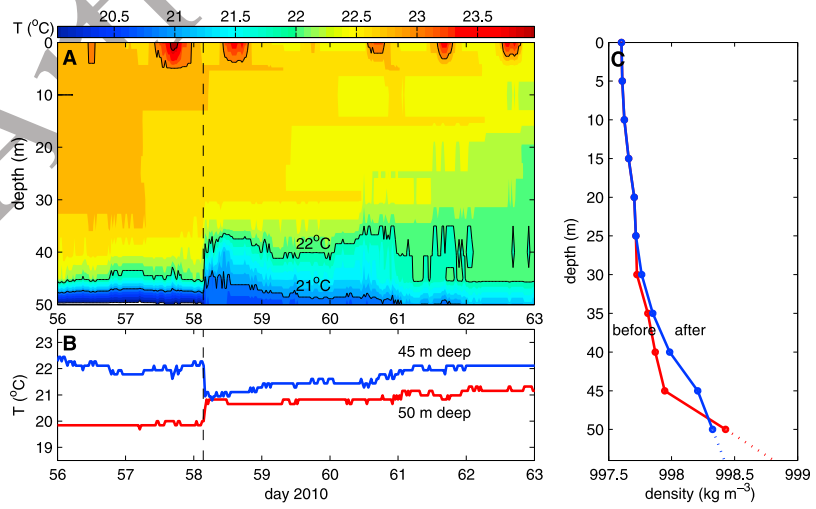

Figure 2. (a) Contour of temporal evolution of vertical profiles of water temperature recorded by the thermistor chain during Maule earthquake (day 58 of 2010). (b) Time series of water temperature measured at 45 m (blue line) and 50 m (red line) depth. Vertical dashed line in Figures 2a and 2b mark the Maule earthquake. (c) Vertical profiles of water density before and after Maule earthquake. Profiles were measured separated each other by 30 min. Dashed line extrapolate measurements toward the bottom of the reservoir at 54 m.

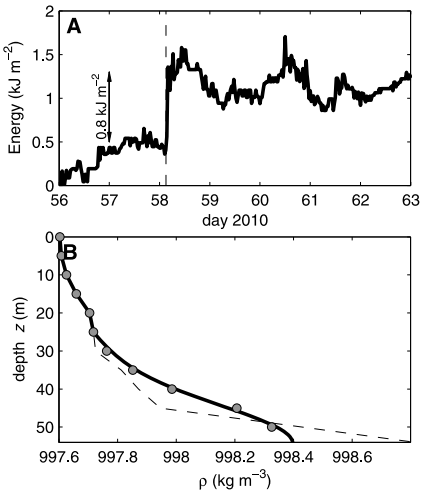

Figure 3. (a) Time series of computed potential energy per unit of area based on water temperature measurements. Vertical dashed line marks the Maule earthquake. (b) Vertical profiles of water density before the earthquake (dashed line), after the earthquake (dots), and simulated after the earthquake for $K_\rho = 2.0 \times 10^{-2}$ m^2 s^{-1} (sold line).

water density below the deepest thermistor was linearly extrapolated toward the bottom of the lake (see dashed line in Figure 3b). K_ρ was then calibrated by minimizing the least square error between measured and simulated water density, obtaining $K_\rho = 2.0 \times 10^{-2}$ m^2 s^{-1} and the corresponding profile is shown in Figure 3b. Values for K_ρ in normal conditions without an earthquake varies between 10^{-4} and 10^{-3} m^2 s^{-1} [*MacIntyre et al.*, 1999; *Lorke et al.*, 2002; *Wüest and Lorke*, 2003].

2.2. Mixing Efficiency

[7] Two different approaches are used to estimate the energy per unit of bed area that was delivered by the earthquake to Rapel reservoir: the second problem of Stokes [*Batchelor*, 1967; *Lorke et al.*, 2002], and *Shih et al.* [2005] and *Ivey et al.* [2008] parameterization of mixing in stratified flows.

[8] The second problem of Stokes consist in solving the horizontal velocity parallel to a wall, $u(z,t)$, with z the vertical coordinate and t the time, which is the result of inducing the flow by an oscillatory boundary conditions at the base of $u(0,t) = u_o \cos(\omega t)$, where $u_o$is the amplitude of the oscillation and ω the frequency at which occurs [*Batchelor*, 1967; *Lorke et al.*, 2002]. In this way, shear stresses induces an oscillatory flow in a region characterized by the thickness of the Stokes layer, $d = 2\pi\sqrt{2\nu/\omega}$, above which no horizontal velocities are expected, with ν denoting the water viscosity that is considered to be the turbulent eddy viscosity in the benthic boundary layer [*Lorke et al.*, 2002], and is assumed equal to $K_\rho = 2.0 \times 10^{-2}$ m^2 s^{-1} since the turbulent Prandtl number is close to 1.0 [*Rodi*, 1983; *Pope*, 2000]. Using the velocity profile of the Stokes problem, the work per unit of area of bed, per oscillating period done by the oscillating on the flow is

$$w = \int_0^{2\pi/\omega} \rho\nu \left.\frac{\partial u}{\partial z}\right|_{z=0} u_o \cos(\omega t) dt = \rho u_o^2 \pi \sqrt{\frac{\nu}{2\omega}}. \quad (3)$$

Then, the net energy per unit of area of bed for a monochromatic oscillation, is calculated as the work per period (w, equation (3)) times the number of periods contained on a time T_s, giving:

$$W = \rho u_o^2 T_s \sqrt{\frac{\nu\omega}{8}}. \quad (4)$$

In this way, the net work per unit of area of bed done by the earthquake on the reservoir, W, can be contrasted with the changes in the potential energy of Rapel reservoir produced by the Maule earthquake ($\Delta PE = 0.8$ kJ m^{-2}, Figure 3a), for which it is required knowing T_s, ν, u_o and ω. T_s is assumed equal to the duration of the earthquake (90 s), and $\nu = K_\rho$ as it was previously discussed. The other two variables, u_o and ω, are taken from the accelerometer station located in Melipilla station (see Figure 1a), which is the closest available seismological station of Rapel reservoir (Seismological Service of Universidad de Chile, 2010, http://ssn.dgf.uchile.cl). Land velocities along west–east and south–north axes were computed by integrating in time the accelerations recorded in Melipilla, and long waves were filtered out [*Boore and Bommer*, 2005] by subtracting to the original time series the moving average of the velocity in a time window of 1s. As an example, the resulting time series of ground velocity along the east–west axis is shown in Figure 4a. Furthermore, the energy spectrum of each component of the land velocity was computed, and the specific kinetic energy of the earthquake per unit of frequency, $u_o^2(\omega)$ used in (4), was computed by adding the energy spectrums of the east–west and south–north components of the horizontal land velocity. Then, the exchanged work per unit of frequency per unit of bed area, $W(\omega)$, was computed based on (4), and the corresponding spectral form is shown in Figure 4b ($\nu = K_\rho = 2.0 \times 10^{-2}$ m^2 s^{-1} and $T_s = 90$ s). Finally, the total energy per unit of area of bed that entered to the reservoir (ΔE) was computed by integrating $W(\omega)$ (Figure 4b) in the range of frequencies of the earthquake (between 10^{-1} and 10^2 rad s^{-1}, Figure 4b), obtaining $\Delta E = 25.6$ kJ m^{-2} that is about 32 times larger than ΔPE, which is equivalent to a mixing efficiency of $\gamma_{mix} = \Delta PE(\Delta E)^{-1} = 3.2\%$. It worth noticing that if this estimation

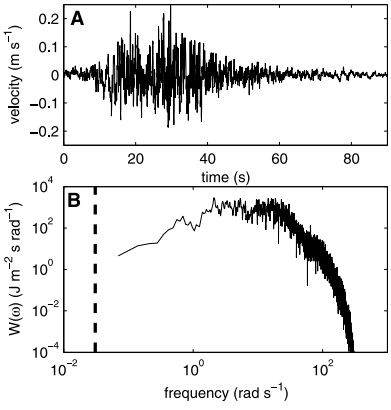

Figure 4. (a) Computed time series of land velocity in Melipilla seismological station, along the West–East direction. (b) Estimated spectral energy per unit of frequency delivered by the earthquake to the reservoir. Vertical dashed line defines maximum buoyancy frequency before the earthquake.

is done by also considering vertical land velocities $\Delta E = 28.3$ kJ m^{-2}, thus showing that in the first approximation the vertical accelerations can be neglected.

[9] The second way of computing the mixing efficiency, γ_{mix}, is based on the results of *Shih et al.* [2005] and *Ivey et al.* [2008]. These authors showed that the energetic regime is described by

$$\frac{K_\rho}{\nu_m} = 2\left(\frac{\varepsilon}{\nu_m N^2}\right)^{0.5} = \gamma_{mix}\left(\frac{\varepsilon}{\nu_m N^2}\right), \quad (5)$$

where ν_m is the molecular kinematic viscosity (1.3×10^{-6} m^2 s^{-1}), N is the buoyancy frequency (rad s^{-1}), and ε is the rate of TKE dissipation (m^2 s^{-3}). Then, using $K_\rho = 2.0 \times 10^{-2}$ m^2 s^{-1},

$$\gamma_{mix} = 4\left(\frac{K_\rho}{\nu_m}\right)^{-1} = 0.03\%. \quad (6)$$

and $\Delta E = \Delta PE\gamma_{mix}^{-1} = 3000$ kJm^{-2} which is equivalent to 24% for a 50 m height water column.

3. Discussion

[10] In this article, we analyzed unique measurements of the hydrodynamic response of Rapel reservoir due to the 8.8 M_w earthquake that hit Central Chile in February 2010. Based on these measurements, the mixing was characterized by a change in the potential energy per unit of area of bed, $\Delta PE = 0.8$ kJm^{-2}, with an eddy diffusivity of $K_\rho = 2.0 \times 10^{-2}$ m^2 s^{-1}, and a mixing efficiency that varied between 0.03 to 3%. Although changes in the potential energy per unit of area of the bed were calculated from the measurements of the thermistor chain, several assumptions were required to estimate both the eddy diffusivity and mixing efficiency.

[11] First of all, to estimate the eddy diffusivity it was required to define the timescale in which mixing occurred, which is something in between the earthquake duration (90 s) and 30 min that is the time-step of the measurements. Previous studies showed that diffusion timescale of turbulent patches $4N^{-1}$ [*Fernando*, 1988] is equal to 13.6 min, when a vertically averaged N is used. However, this timescale is valid for three-dimensional turbulent patches, while the turbulence induced by the earthquake is bounded by the bottom of the reservoir.

[12] Second, it was assumed that the vertical mixing was driven by the turbulent flow induced in the benthic boundary layer by the oscillation of the bed. Questions arise whether or not this was the only mixing mechanism excited by the earthquake. The excitation of surface and internal waves is a plausible hypothesis for also explaining the observed increase in vertical mixing, as the benthic boundary is usually energized by shear-induced turbulence or by internal wave breaking [*Gloor et al.*, 2000; *Boegman et al.*, 2003; *Lorke et al.*, 2005]. To preliminarily define whether the excitation of surface and internal waves by the earthquake is possible, it is considered that only those waves with natural frequencies near the earthquake frequency are likely to be excited, thus neglecting nonlinear energy transfers among waves as a mechanism of excitation [*de la Fuente et al.*, 2010]. With this consideration in mind, internal waves are not possible to be excited because the oscillations induced by the earthquake delivered energy in flow-scales of $\omega = 10$ rad s^{-1}, which are faster than the buoyancy frequency (vertical line in Figure 4b) that defines the higher frequency at which a stratified fluid oscillates [*Boegman et al.*, 2003]. Surface waves, in contrast, are much faster than the internal waves, thus being more likely to be excited by the land oscillations of the earthquake. In this case, the wavelength, L, of a gravitational surface waves excited by an oscillating forcing can be estimated as

$$L = \frac{2\pi}{\omega}c \quad (7)$$

where $c = \sqrt{gh}$ is the surface wave celerity of a water column with a depth h. With $h = 54$ m and $\omega = 10$ rad s^{-1}, the wavelength is $L = 14.5$ m, which are small waves rather than basin-scale waves. However, because available measurements are every 30 minutes, it is unclear if surface waves were excited by the earthquake, and how much energy flood into them.

[13] Third, the mixing efficiency, γ_{mix}, was estimated with the second problem of Stokes, obtaining $\gamma_{mix} = 3.2\%$; and with *Shih et al.* [2005] and *Ivey et al.* [2008] parameterization of mixing for stratified flows, obtaining $\gamma_{mix} = 0.03\%$, which have a difference of two-order of magnitude. The problem is that neither of these two approaches is actually valid for the conditions of the earthquake. On the one hand, the Stokes solution is valid for a constant and homogeneous ν. On the other hand, equations (5) and (6) are valid for $\varepsilon(\nu_m N^2)^{-2} < 10^6$, whereas during the earthquake $\varepsilon(\nu_m N^2)^{-1} \sim O(10^8)$. Further research is needed to elucidate this issue.

[14] **Acknowledgments.** We wish to thank to Francisco Ortega, Sergio Ruiz, and Pedro Soto for their support in processing seismological data, and Carlos Rozas for his helpful comments on an early version of this paper.

References

Antenucci, J. P., J. Imberger, and A. Saggio (2000), Seasonal evolution of the basin-scale internal wave field in a large stratified lake, *Limnol. Oceanogr.*, *45*, 1621–1638, doi:10.4319/lo.2000.45.7.1621.

Batchelor, G. K. (1967), *An Introduction to Fluid Dynamics*, Cambridge Univ. Press, Cambridge, U. K.

Boegman, L., J. Imberger, G. N. Ivey, and J. P. Antenucci (2003), High-frequency internal waves in large stratified lakes, *Limnol. Oceanogr.*, *48*, 895–919, doi:10.4319/lo.2003.48.2.0895.

Boore, D. M., and J. J. Bommer (2005), Processing of strong-motion accelerograms: Needs, options and consequences, *Soil. Dyn. Earthquake Eng.*, *25*, 93–115, doi:10.1016/j.soildyn.2004.10.007.

Contreras, M., H. Villagran, and C. Salazar (1994), Hydrodynamic characteristics of Rapel reservoir (in Spanish), *Medio Ambiente*, *12*, 41–49.

de la Fuente, A., and Y. Niño (2008), Pseudo 2D ecosystem model for a dendritic reservoir, *Ecol. Modell.*, *213*, 389–401, doi:10.1016/j.ecolmodel.2008.01.020.

de la Fuente, A., K. Shimizu, Y. Niño, and J. Imberger (2010), Nonlinear and weakly non-hydrostatic inviscid evolution of internal gravitational basin-scale waves in a large, deep lake: Lake Constance, *J. Geophys. Res.*, doi:10.1029/2009JC005839, in press.

Farías, M., G. Vargas, A. Tassara, S. Carretier, S. Baize, D. Melnick, and K. Bataille (2010), Land-level changes produced by the Mw8.2 2010 Chilean Earthquake, *Science*, doi:10.1126/1192094, in press.

Fernando, H. J. S. (1988), The growth of a turbulent patch in a stratified fluid, *J. Fluid Mech.*, *190*, 55–70, doi:10.1017/S002211208800120X.

Fischer, H., E. List, R. Koh, J. Imberger, and N. Brooks (1979), Mixing, in *Inland and Coastal Waters*, Academic, San Diego, Calif.

Gloor, M., A. Wüest, and D. M. Imboden (2000), Dynamics of mixed bottom boundary layers and its implications for diapycnal transport in a stratified, natural water basin, *J. Geophys. Res.*, *105*, 8629–8646, doi:10.1029/1999JC900303.

Imberger, J., and P. F. Hamblin (1982), Dynamics of lakes, reservoirs and cooling ponds, *Annu. Rev. Fluid Mech.*, *14*, 153–187, doi:10.1146/annurev.fl.14.010182.001101.

Ivey, G. N., K. B. Winters, and J. R. Koseff (2008), Density stratification, turbulence, but how much mixing?, *Annu. Rev. Fluid Mech.*, *40*, 169–184, doi:10.1146/annurev.fluid.39.050905.110314.

Kaiser, J., and A. Regalado (2010), Chile's earthquake may set back research for years, *Science*, *327*, 1308–1309, doi:10.1126/science.327.5971.1308.

Lay, T., C. J. Ammon, H. Kanamori, K. D. Koper, O. Sufri, and A. R. Hutko (2010), Teleseismic inversion for rupture process of the 27 February 2010 Chile (M_w 8.8) earthquake, *Geophys. Res. Lett.*, *37*, L13301, doi:10.1029/2010GL043379.

Lorke, A., L. Umlauf, T. Jonas, and A. Wüest (2002), Dynamics of turbulence in low-speed oscillating bottom-boundary layers of stratified basins, *Environ. Fluid Mech.*, *2*, 291–313, doi:10.1023/A:1020450729821.

Lorke, A., F. Peeters, and A. Wüest (2005), Shear-induced convective mixing in bottom boundary layers on slopes, *Limnol. Oceanogr.*, *50*, 1612–1619, doi:10.4319/lo.2005.50.5.1612.

MacIntyre, S., K. M. Flynn, R. Jellison, and J. R. Romero (1999), Boundary mixing and nutrient fluxes in Mono Lake, California, *Limnol. Oceanogr.*, *44*, 512–529, doi:10.4319/lo.1999.44.3.0512.

Madariaga, R., M. Métois, C. Vigny, and J. Campos (2010), Central Chile finally breaks, *Science*, *328*, 181–182, doi:10.1126/science.1189197.

Montgomery, D. R., and M. Manga (2003), Streamflow and water well responses to earthquakes, *Science*, *300*, 2047–2049, doi:10.1126/science.1082980.

Patankar, S. V. (1980), *Numerical Heat Transfer and Fluid Flow*, McGraw-Hill, New York.

Pope, S. (2000), *Turbulent Flows*, Cambridge Univ. Press., Cambridge, U. K.

Regalado, A. (2010), Scientists count the coasts of Chile's quake, *Science*, *328*, 157, doi:10.1126/science.328.5975.157-b.

Rodi, W. (1983), *Turbulence Models and Their Application in Hydraulics; A State-of-the-Art Review*, IAHR, Delft, Netherlands.

Shih, L. H., J. Koseff, G. N. Ivey, and J. H. Ferziger (2005), Parameterization of turbulent fluxes and scales using homogeneous sheared stably stratified turbulence simulations, *J. Fluid Mech.*, *525*, 193–214, doi:10.1017/S0022112004002587.

Shimizu, K., and J. Imberger (2008), Energetics and damping of basin-scale internal waves in a strongly stratified lake, *Limnol. Oceanogr.*, *53*, 1574–1588, doi:10.4319/lo.2008.53.4.1574.

Shimizu, K., J. Imberger, and M. Kumagai (2007), Horizontal structure and excitation of primary motions in a strongly stratified lake, *Limnol. Oceanogr.*, *52*, 2641–2655, doi:10.4319/lo.2007.52.6.2641.

Vila, I., M. Contreras, V. Montecinos, J. Pizarro, and D. Adams (1997), Rapel: A 30 years temperate reservoir. Eutrophication or Contamination?, *Arch. Hydrobiol. Spec. Issues Advanc. Limnol.*, *55*, 31–44.

Wüest, A., and A. Lorke (2003), Small-scale hydrodynamics on lakes, *Annu. Rev. Fluid Mech.*, *35*, 373–412, doi:10.1146/annurev.fluid.35.101101.161220.

Wüest, A., G. Piepke, and D. C. Van Senden (2000), Turbulent kinetic energy balance as a tool for estimating vertical diffusivity in wind-forced stratified waters, *Limnol. Oceanogr.*, *45*, 1388–1400, doi:10.4319/lo.2000.45.6.1388.

M. Contreras, Centro de Ecología Aplicada Ltda., Avenida Suecia 3304, Santiago, Chile.

A. de la Fuente, Y. Niño, and H. Ulloa, Departamento de Ingeniería Civil, Universidad de Chile, Avenida Blanco Encalada 2002, Santiago, Chile. (aldelafu@ing.uchile.cl)

C. Meruane, Ingeniería y Modelación Ambiental Ltda., Calle Loreley 1023, Santiago, Chile.